Analysis of non-ideal remote pole in Electrical Resistivity Tomography for subsurface surveys

Gabriele Patrizi [1] *, Giulia Guidi [1], Lorenzo Ciani [1], Marcantonio Catelani [1], Luca Cappuccini [2], Agnese Innocenti [3], Nicola Casagli [3], Veronica Pazzi [4, 3]

[1] *Dept. of Information Engineering*, *University of Florence,* via di S. Marta 3, 50139, Florence (IT)
[2] *Dept. of History, Archaeology, Geography, Fine and Performing* Arts, *University of Florence*, Via San Gallo 10, 50124 Florence (IT)
[3] *Department of Earth Sciences, University of Florenze*, Via G. La Pira 4, 50121 Florence (IT)
[4] *Dept. of Mathematics and Geosciences, University of Trieste*, via Weiss 4, 34128 Trieste (IT)
* Corresponding author (Gabriele Patrizi): gabriele.patrizi@unifi.it

***Abstract* — One of the most used geophysical measurement techniques for soil reconstruction is the Electrical Resistivity Tomography. In many different application fields, the reconstruction of the subsurface must be accurate and precise in order to properly identify the underground target. In many practical cases this will allow to decrease the costs thanks to an easier and more accurate plan of the excavation survey. There are different array geometries that could be used in Electrical Resistivity Tomography depending on the area of investigation. Some of them uses a remote electrode (also known as remote pole) ideally located at infinite distance from the other electrodes. Obviously, since the length of the cable is finite, it is not possible to deploy the remote pole at the theoretical infinite distance. Thus, it is fundamental to understand how this error influence the subsurface reconstruction. Starting from a previous work, this paper compares the output of a Monte Carlo simulation with the results of a measurement survey carried out on an Etruscan tumulus. The location of the remote pole has been changed starting at 50 m up to 150 m from the center of the linear array. The results of both simulations and measurement campaign emphasizes the effects of a non-ideal remote pole in terms of apparent resistivity of the subsurface and colormap-based soil reconstruction.**

Keywords — Archeological survey; Geophysical measurements; Remote Pole; Resistivity measurements; Soil reconstruction; Subsurface resistivity.

I. Introduction

Electrical Resistivity Tomographies (ERTs) are widely used in many investigation fields (e.g., environmental characterization, engineering geology, hydrogeology, civil engineering, waste investigations, and archaeology. See [1] and references therein). Despite the successes of the ERT method as non-invasive geophysical technique, the accurate resolution in identifying buried objects depth and dimensions strongly depends on the electrodes' spatial distribution (array) over the surface [2]–[6].

Different arrays (i.e., different reciprocal position of the current and voltage electrodes) have different resolutions, and each array has its advantages and limitations. A comparison among the 10 most employed array configuration is presented in [7]. Here the characteristics of the Pole-Dipole (PD), the one employed in this work, are the only one presented. Compared to the other arrays, PD has a higher spatial resolution capacity and penetration depth, even it is more susceptible to noise contamination; therefore, it represents a suitable compromise between resolution and signal strength.

Nevertheless, one of the main disadvantages of the PD array is linked to the array geometry itself, i.e., the position of one of the two current electrodes theoretically must be at infinity, but this theoretical infinite location (the so-called remote pole) is difficult to achieve in the field.

Starting from the consideration that many authors do not take into account the real finite location of the remote pole, thinking that inversion results are not really affected by considering at infinity what it is not, Razafindratsima & Lataste in [8] compared the result of model and field survey carried out with both theoretical and real remote pole position. They concluded that it is always better to use the real remote pole position instead of putting it at theoretic infinite distance. Therefore, since the finite cable length does not allow to place the remote pole at the theoretical infinite distance, the PD array is systematically affected by the electrode-spacing errors as defined by Zhou & Dahlin in [9] or mislocation error as stated by Oldenborger et al. in [10].

In their work Razafindratsima & Lataste [8] also demonstrated the following:

a) that to reduce at the minimum the effects of the finite location of the remote pole this has to be placed at least at a minimum distance, that depend on the maximum quadripole aperture;

b) that the induced error is related to the angle between the three in-line electrodes and the line that join the remote pole and the last voltage electrode.

In a previous work published in [11] a Monte Carlo simulation analysis has been used to demonstrate that to minimize the effects of a finite remote pole position, it should be located perpendicularly to the center of the ERT line, and at a distance at least equal to the length of the whole line itself. Moreover, the study suggests that it is not necessary to reach further location since the geometric factor remains almost the same. To further develop this previous research, this paper reports the results of a measurement campaign using a PD array and different remote pole locations. The aim of the work is to validate the simulations carried out in [11] emphasizing the effects of a non-ideal remote pole using the results achieved on the survey. Varying the distance from the remote pole to the center of the array the measured resistivity and the colored image reconstruction of the subsurface are used to validate the results of the simulation.

The rest of the paper is organized as follow: section II presents a brief overview of the pole-dipole array and remote pole positioning, section III describes the area of investigation and the measurement survey while the results have been detailly discussed section IV.

II. Brief overview of Pole-Dipole Array

The aim of ERT technique is to characterize the resistivity of the ground at various depths of investigation starting from current and voltage measurements on the soil surface. A specific instrument uses a set of numerous electrodes to measure the "apparent resistivity". This variable is called apparent since it is achieved assuming a homogeneous structure of the soil. Then, the results of the apparent resistivity along with the array geometry and the actual GPS coordinates of the electrodes are used to solve the "inversion problem" generating a colored image of the subsurface, where the color map represents different values of the actual resistivity of the subsurface [12], [13].

The Pole-Dipole array is a common geometry used in many different ERT applications. In compliance with [11] an example of acquisition using PD array is illustrated in Fig. 1.

The electrodes A and B are called current electrodes or current dipole because they are used to generate a DC voltage of hundreds of Volt and then measure the current that flows through the ground between them (identified as I_{AB} in the following). The remote pole B is fixed and common to every acquisition. It should be located perpendicular to the linear array, at theoretical infinite distance [11]. The electrodes M and N are called voltage electrodes or voltage dipole because they are used to measure the potential difference (identified as ΔV_{MN} in the following) in a certain point of the array induced by the DC voltage generated between A and B. Repeating this measure toward a line, with different extensions of the dipoles and different distance between them it is possible to investigate the resistivity of the soil from the surface up to a depth that depend on the maximum quadripole aperture. In order to do that, the geometric factor k and the apparent resistivity ρ are given by [14]:

$$\mathrm{k} = \frac{2\pi}{\left(\frac{1}{\overline{\mathrm{AM}}} - \frac{1}{\overline{\mathrm{BM}}} - \frac{1}{\overline{\mathrm{AN}}} + \frac{1}{\overline{\mathrm{BN}}}\right)} \quad (1)$$

$$\rho = \mathrm{k}\frac{\Delta \mathrm{V}}{\mathrm{I}} \quad (2)$$

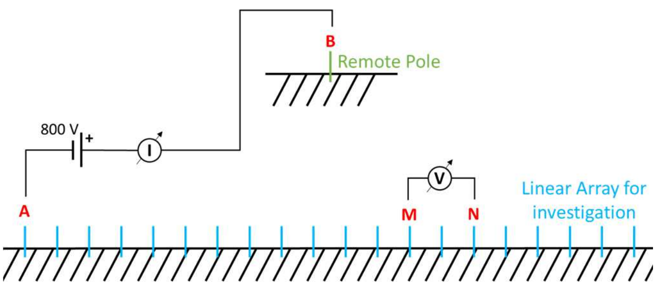

Fig. 1. Example of ERT investigation using Pole-Dipole array. The blue line are the standard electrodes, while the green line stands for the remote pole.

III. Area of Investigation

In order to fulfill the aim of the work an ERT survey has been carried out using the Pole-Dipole array geometry on a site of archeological interest. The Poggio Pepe tumulus has a diameter of about 90 m and is the fifth largest tumulus known in Tuscany. It is located North-East of Vetulonia town (Tuscany, central Italy), one of the most important Etruscan towns of 6th century BC. From a geological point of view, the Poggio Pepe tumulus is characterized by the Macigno unit sandstones (Upper Oligocene/Lower Miocene). Shales and limestones of Canetolo unit (Paleocene/Eocene) can be found in the western part of the tumulus, while holocenic slope deposits, with limited thickness, in the northern and southern part of the area. For more details on the study area see [15], [16].

The measurement campaign has been carried out using 72 electrodes linearly displaced at 1 m distance from each other. This type of array allows to acquire 2D data about the subsurface resistivity beneath the array up to 20 m depth. In order to do that, 2625 acquisitions in sequence have been performed by the instrument changing the A, M and N electrodes among the 72 linearly displaced. The remote pole has been located perpendicular to the array. The measurement campaign has been repeated varying the distance of the remote pole from the center of the array as follow: 50 m, 100 m and 150 m.

The coordinates of the electrodes (blue dots) and the coordinates of the remote poles are illustrated in Fig. 2 using the WGS84 coordinate system.

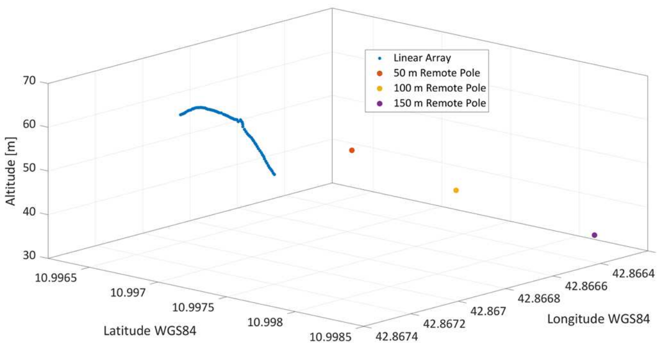

Fig. 2. Representation of the Pole-Dipole array used in the measurement campaign highlighting the different distances of the remote poles.

IV. Results and Discussion

This section compares the output of the simulations against the results achieved during the measurement campaign carried out on the Poggio Pepe tumulus.

The optimal positioning of the remote pole has been identified in a previous work published in [11]. Using Monte Carlo simulations, the paper emphasizes the necessity to deploy the remote pole perpendicularly to the array. The distance from the center of the array should be at least equal to the total length of the array. Such considerations are clearly visible in Fig. 3, where the geometric factor of the different acquisitions carried out on the survey is illustrated.

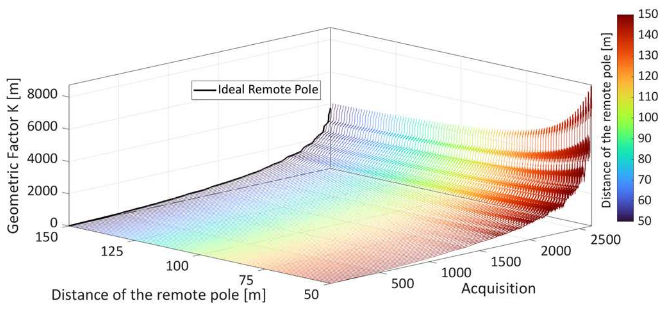

Fig. 3. Simulation of the Geometric factor for the considered survey varying the distance of the remote pole from 50 m up to 150 m.

The black thick line represents the ideal geometric factor simulated assuming a remote pole deployed infinitely distant from the array. The thin colored lines stand for the real remote pole, simulated varying the distance from 50 m up to 150 m from the center of the array. All the curves of the geometric factor in Fig. 3 have been sorted in ascending order, which means that the greater the number of acquisitions, the greater the geometric factor and thus the deeper the section of investigation.

What stands out from Fig. 3 confirms the fact that is fundamental to locate the remote pole at a distance at least equal to the total length of the array. As a matter of fact, considering the simulations carried out with distance greater than 110 - 120 m, the results are quite similar to the simulation performed with the ideal remote pole deployed at infinite position. Only a minor error has been identified in such cases, leading to a neglectable difference in terms of apparent resistivity and actual resistivity.

Quite the opposite, if the distance of the remote pole is comparable with the total length of the array (71 m in this measurement campaign) it is not possible to neglect the error due to the non-ideality of the remote pole. Moreover, it is important to point out that the distance of the remote pole mostly affect the acquisitions carried out at greater depth (i.e., higher number of acquisition). However, the appearing of this phenomenon is moving toward shallow depths when the distance of the remote pole keeps reducing.

To validate the results achieved with the proposed simulations, the following part of the section illustrates the results of the measurement campaign carried out using three different positions of the remote pole: 50 m, 100 m, and 150 m respectively moving linearly and perpendicularly from the center of the array.

The raw data acquired by the instrument in the three scenarios previously mentioned are illustrated in Fig. 4, where different colors have been used to identify the different sequences of acquisition. The measured apparent resistivity plotted in Fig. 4 has been ordered by increasing depth of investigation in order to emphasize the effects that the position of the remote pole has at different depths.

What stands out from the figure is that in the first 1500 acquisitions (i.e., shallow depths) the three sequences of data are practically the same. However, increasing the depth of investigation, the blue (i.e., distance equal to 50 m) and red (i.e., distance equal to 100 m) lines start presenting some peaks and alterations with respect to the acquisitions carried out using the remote pole deployed at 150 m (i.e., green line).

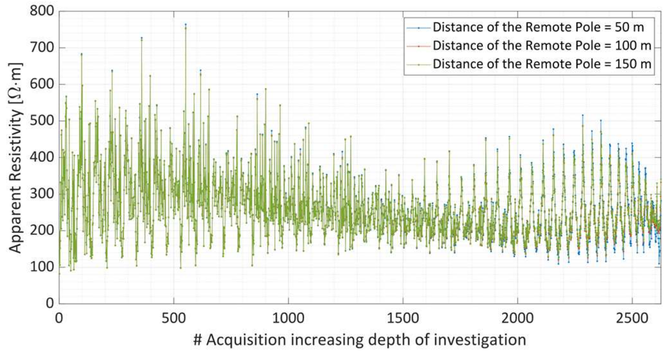

Fig. 4. Results of the measurement campaign for three different distances of the remote pole. The apparent resistivity acquired by the instrument has been ordered by increasing depth of investigation.

In order to properly quantify the effects of the non-ideal infinite position of the remote pole, an adequate figure of merit has been introduced. In particular, the percentage relative error at 50 m Γ_{50} as in equation (3) has been calculated as the difference between the ideal geometric factor located at infinite position (i.e., K_∞ in the following) and the actual geometric factor K_{50} evaluated using the actual position of the remote pole deployed at 50 m from the center of the array, as follow:

$$\Gamma_{50} = 100 \cdot \left|\frac{K_\infty - K_{50}}{K_\infty}\right| \quad (3)$$

Similarly, the percentage relative error in case of 100 m (i.e., Γ_{100}) and 150 m (i.e., Γ_{150}) remote pole distances are given by:

$$\Gamma_{100} = 100 \cdot \left|\frac{K_\infty - K_{100}}{K_\infty}\right| \quad (4)$$

$$\Gamma_{150} = 100 \cdot \left|\frac{K_\infty - K_{150}}{K_\infty}\right| \quad (5)$$

The percentage relative error Γ_{50}, Γ_{100}, and Γ_{150} have been evaluated for every acquisition carried out during the measurement survey. The results are illustrated in Fig. 5, where each subplot represents a different distance of the remote pole location from the center of the array. Also in this case, the plotted values have been sorted for increasing depth of investigation. Furthermore, a color-based line has been used to rapidly and clearly understand the depth of investigation of each acquisition. This is extremely helpful to understand the effects of a non-ideal remote pole when the depth of analysis increases.

Analyzing the results in Fig. 5 it is possible to validate the output of the simulations reported in Fig. 3. More in detail, the top subplot highlights the severe impact of a closely located remote pole. When the distance from the center of the array is only 50 m the percentage relative error rapidly increases reaching values of over 150% at 20 m depth. The top subplot also emphasizes that this kind of remote pole provides reliable and trustworthy results only up to approximately 5 m depth. After that, the non-ideality could not be neglected any more. Slightly better results have been obtained in case of 100 m distance of the remote pole, as in the middle subplot in Fig. 5.

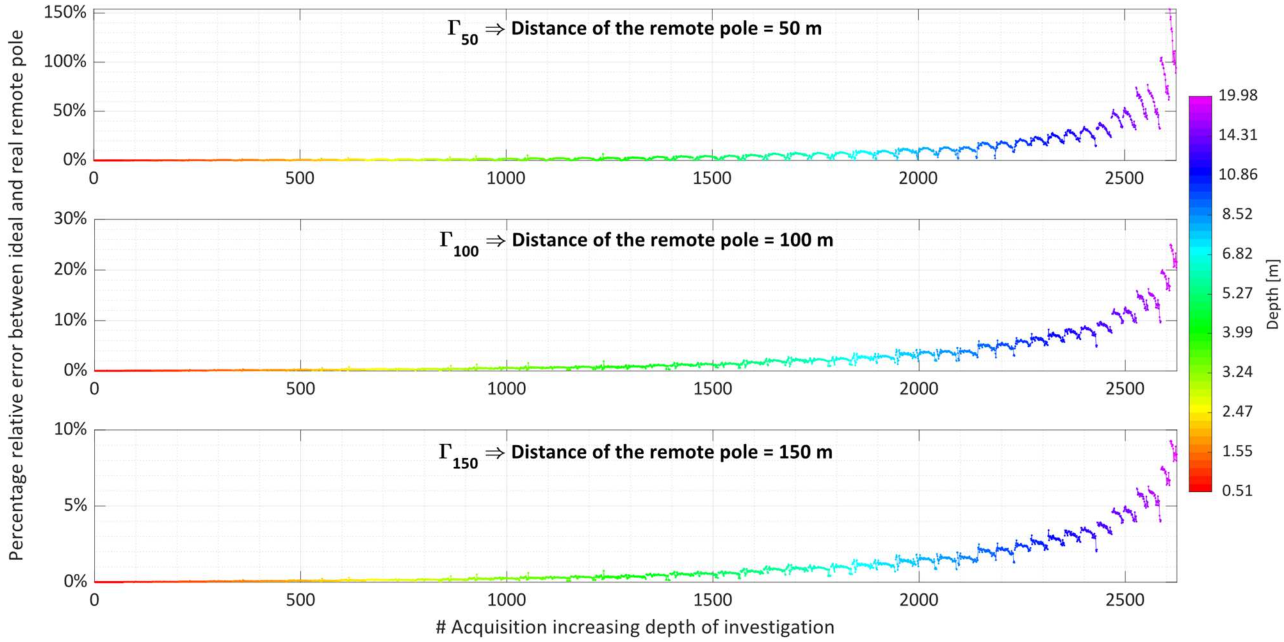

Fig. 5. Percentage relative error sorted increasing the depth of investigation according to the colobar on the right side of the image. Each sublot illustrates the results of a different measurement survey performed using different remote poles.

In fact, in case of Γ_{100}, the maximum error in terms of apparent resistivity is approximately 25 % at 20 m depth, and only measurement carried out deeper than 14 m are characterized by percentage errors greater than 12%.

The best scenario is represented by the bottom subplot in Fig. 5, where Γ_{150} refers to a distance of the remote pole equal to 150 m. This allows to keep the percentage relative error below the 9% at any investigated depth and below the 5% up to 15 m depth.

Finally, Fig. 6 shows the results of the measurement campaign in terms of actual resistivity of the subsurface after solving the inversion problem and starting from the results of the survey illustrated in Fig. 4.

The different resistivity values in Fig. 6 are illustrated using different colors, according to the colorbar on the right side of the image. The image takes into account the actual profile of the investigated hill and the real positions of the 72 linearly displaced electrodes (red dots on the top side of each subplot). For the sake of readability, the remote pole is not illustrated in the image.

What stands out from a first rough analysis of the figure is that there is not a remarkable difference between the three surveys carried out with different remote poles. As a matter of fact, moving forward from the apparent resistivity of the homogeneous soil (i.e., the raw data acquired by the instrument) to the actual resistivity of the subsurface (i.e., the colormap in Fig. 6) the effects of a non-ideal remote pole considerably decrease. An effective inversion algorithm is able to mitigate the negative effect of a too-closely located remote pole. As you can see, at great depth the actual resistivity measured using the remote pole located at 50 m is lower than the other cases (darkest shades of blue). Such low levels of resistivity are indicative of the presence of homogeneous clay rich subsoil. Thus, since no target are present in that area, the error due to the non-ideal remote pole is negligible.

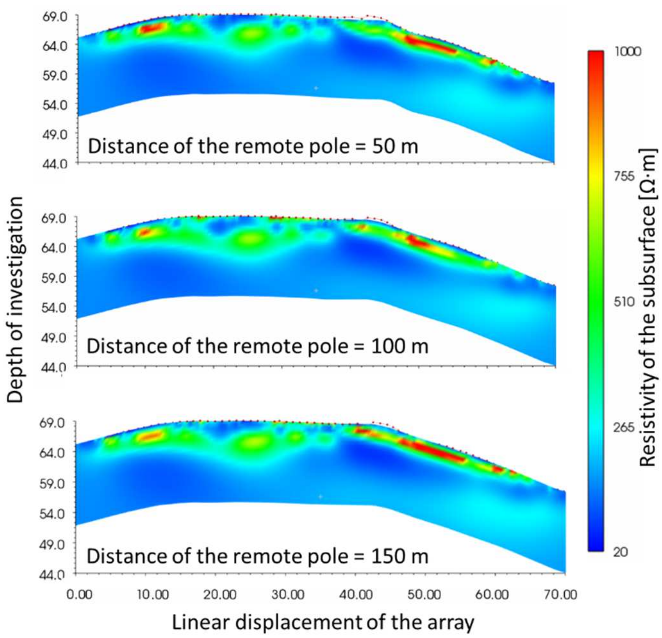

Fig. 6. Colored image of the reconstructed subsurface in case of 50 m, 100 m and 150 m distance of the remote pole. The image has been achieved after solving the inversion problem.

Quite differently, some alterations are still present in case of 50 m and 100 m distance with respect to the almost-ideal 150 m distance in the areas where some resistivity anomalies are present. Looking at the figures, it is possible to identify three different resistivity anomalies (i.e., resistivity values greater than or equal to 500 Ωm represented using green, yellow, and red). Moving from the left to the right of the figure, the first anomaly is in correspondence of a monumental staircase brought to light during the 2020 excavation campaign. Thus, it could indicate a portion of the staircase still buried. By a measurement analysis, it is possible to see that in case of a too-close remote pole the position of the anomaly slightly change and the resistivity reaches higher values with respect to the bottom subplot (i.e., distance of the remote pole equal to 150 m). The second anomaly is located approximately on the center of the array and because of its dimension and the resistivity values it could represent the funeral chamber filled whether with soil or air. In this case the effect of the remote pole in the top subplot is the opposite and the resistivity of the anomaly is slightly lower than the bottom subplot. The third anomaly, located on the right side of the image, is probably caused by the presence of rocky masses accumulated there in quite recent years during the ploughing activity. The topographic anomaly located between 47 m and 53 m, in fact, is caused by a hedge used to delimit two different properties. In this case, the effects of a non-correct positioning of the remote pole are the most critical. As you can see comparing the top and bottom subplots, the dimension of this anomaly remarkably increases increasing the distance of the remote pole. This means that, if the acquisitions are carried out only with the lower distance of the remote pole, this could lead to severe mistakes in the excavation process.

In summary, by a macroscopic point of view the effects of a non-ideal remote pole in terms of variation of the actual resistivity of the subsurface are mitigated by the inversion algorithm. However, even if the impact decreases with respect to the apparent resistivity, some alterations are still present in the most critical zones of the subsurface. As a matter of fact, if the remote pole is not located at a distance at least comparable with two times the length of the array the error committed in presence of resistivity anomalies is not affordable.

Conclusions

This work is based on a ERT measurement survey carried out on the Etruscan tumulus of Poggio Pepe (central Italy) to investigate the effects of a non-correct positioning of the remote pole in Pole-Dipole linear array. Literature highlights that the remote pole should be located perpendicular to the center of the array, at theoretical infinite distance. Since this ideal scenario could not be achieved because of the finite length of the connection cable, it is extremely important to investigate the effects of a non-ideal remote pole in terms of both apparent resistivity of the homogeneous ground (i.e., the raw data acquired by the instrument) and actual resistivity of the subsurface. The first part of the experimental analysis deals with the simulation of the geometric factor using a remote pole distance in the range from 50 m to 150 m and comparing the results with the ideal geometric factor achieved considering an infinite distance of the remote pole. Then, the results of the experimental survey carried out on the tumulus have been used to validate the output of the simulations. If the remote pole distance is comparable with the length of the array the percentage relative error between measurements and ideal scenario reaches over 150% at great depth of investigation. Such error decreases of more than 6 times increasing the distance of the remote pole up to two times the length of the array (almost 150 m in the considered survey). Additionally, the effects of the non-ideal remote pole have been investigated also in the colored image reconstruction of the subsurface. In this case, by a macroscopic point of view the error is slightly decreased. However, there are few zones in the reconstructed subsoil where the effects still remain considerable. In presence of resistivity anomalies, if the remote pole is located too close to the array, misleading result in the colored image are present, leading to a non-optimal management of the excavation.

References

[1] V. Pazzi *et al.*, "Analysis of the Influence of the GPS Errors Occurred While Collecting Electrode Coordinates on the Electrical Resistivity of Tumuli," *Sensors 2020, Vol. 20, Page 2966*, vol. 20, no. 10, p. 2966, May 2020.

[2] L. Busato *et al.*, "Combined geophysical surveys for the characterization of a reconstructed river embankment," *Eng. Geol.*, vol. 211, pp. 74–84, Aug. 2016.

[3] T. Herring, L. J. Heagy, A. Pidlisecky, and E. Cey, "Hybrid parametric/smooth inversion of electrical resistivity tomography data," *Comput. Geosci.*, vol. 159, p. 104986, 2022.

[4] Y. Ahn, M. Han, and J. Choi, "Effect of electrode types and soil moisture on the application of electrical resistivity tomography and time-domain induced polarization for monitoring soil stabilization," *Measurement*, vol. 187, p. 110220, Jan. 2022.

[5] A. Getaneh and T. Haile, "Optimized electrical resistivity tomography investigation established in identifying pit tombs of Mogareb, a cemetery area in a Pre-Aksumite archaeological site of Seglamen, northern Ethiopia," *Measurement*, vol. 129, pp. 558–564, Dec. 2018.

[6] F. Li, F. Dong, and C. Tan, "Landweber Iterative Image Reconstruction Method Incorporated Deep Learning for Electrical Resistance Tomography," *IEEE Trans. Instrum. Meas.*, vol. 70, pp. 1–11, 2021.

[7] T. Dahlin and B. Zhou, "A numerical comparison of 2D resistivity imaging with 10 electrode arrays," *Geophys. Prospect.*, vol. 52, no. 5, pp. 379–398, Sep. 2004.

[8] S. Razafindratsima and J.-F. Lataste, "Estimation of the error made in Pole–Dipole Electrical Resistivity Tomography depending on the location of the remote electrode: Modeling and field study," *J. Appl. Geophys.*, vol. 100, pp. 44–57, 2014.

[9] B. Zhou and T. Dahlin, "Properties and effects of measurement errors on 2D resistivity imaging surveying," *Near Surf. Geophys.*, vol. 1, no. 3, pp. 105–117, Aug. 2003.

[10] G. A. Oldenborger, P. S. Routh, and M. D. Knoll, "Sensitivity of electrical resistivity tomography data to electrode position errors," *Geophys. J. Int.*, vol. 163, no. 1, pp. 1–9, Oct. 2005.

[11] L. Ciani *et al.*, "Comparing the Effects of GPS Error on Different Electrical Resistivity Tomography Arrays for Archeological Investigations," *IEEE Trans. Instrum. Meas.*, vol. 70, pp. 1–12, 2021.

[12] L. Zhang, H. Wang, and Y. Xu, "A shrinkage-thresholding method for the inverse problem of Electrical Resistance Tomography," in *2012 IEEE International Instrumentation and Measurement Technology Conference Proceedings*, May 2012, pp. 2425–2429.

[13] F. Li, C. Tan, and F. Dong, "Electrical Resistance Tomography Image Reconstruction With Densely Connected Convolutional Neural Network," *IEEE Trans. Instrum. Meas.*, vol. 70, pp. 1–11, 2021.

[14] D. D. Werkema, E. Atekwana, W. Sauck, and J. A. Asumadu, "A generic automated/semiautomated digital multi-electrode instrument for field resistivity measurements," *IEEE Trans. Instrum. Meas.*, vol. 49, no. 6, pp. 1249–1253, 2000.

[15] M. Catelani *et al.*, "Effects of inaccurate electrode positioning in subsurface resistivity measurements for archeological purposes," in *2021 IEEE International Instrumentation and Measurement Technology Conf (I2MTC)*, May 2021, pp. 1–6.

[16] V. Pazzi *et al.*, "ERT investigation of tumuli: does the errors in locating electrodes influence the resistivity?," in *2019 IMEKO TC-4 International Conference on Metrology for Archaeology and Cultural Heritage*, 2019, pp. 527–532.